Process development exploiting competitive adsorption-based displacement effects in monoclonal antibody aggregate removal—A new high-throughput screening procedure for membrane chromatography

Dominik Stein[1,2] | **Volkmar Thom[1]** | **Jürgen Hubbuch[2]**

[1] Sartorius Stedim Biotech GmbH, Goettingen, Germany

[2] Department of Engineering in Life Sciences, Section IV: Biomolecular Separation Engineering, Karlsruhe Institute of Technology (KIT), Karlsruhe, Germany

Correspondence
Dominik Stein, Sartorius Stedim Biotech GmbH, August-Spindler-Str. 11, Goettingen D-37079, Germany.
Email: Dominik.Stein@Sartorius.com

Abstract

High-throughput screening (HTS) approaches are commonly used to accelerate downstream process development. Although most HTS approaches use batch isothermal data (K_P screen) or bind and elute mode as screening procedure, different or new process designs are rarely investigated. In this paper, a mechanistic model case study for the separation of two different two-component solutions was conducted and confirmed prior evidence. With these outcomes, a novel HTS screening procedure was developed including the determination of competitive adsorption-based displacement effects and key parameter identification. The screening procedure employing an overload bind and elute (OBE) mode is presented in a case study dealing with IgG aggregate removal in a typical monoclonal antibody purification step, applying a Sartobind® S membrane adsorber (MA). Based on a MA scale down device, the OBE mode allows the determination of classical process parameters and dynamic effects, such as displacement effects. Competitive adsorption-based displacement effects are visualized by introducing a displacement identifier leading to a displacement process map. Based on this map, the approach is transferred to and confirmed by the OBE recycle experiments with 4.6 and 8.2 ml benchtop scsale devices resulting in 45% reduced IgG monomer and 88% increased higher molecular weight species binding capacities.

KEYWORDS
aggregate removal, competitive adsorption, high-throughput screening, membrane chromatography

1 | INTRODUCTION

Downstreamprocess development faces increasing diversity of therapeutic modalities, shortened timelines, high cost, and limited availability of the target entity.[1,2] With regard to the classic purification process, the chromatographic process development is challenged by the following aspects: (a) abundance of different ligands, (b) different stationary phase, (c) a range of potential process parameters, and (d) new process designs resulting in a high experimental effort.[1,3] High-throughput screening (HTS)

on robotic platforms typically addresses the challenges posed by the abundance of the different ligands and a range of possible process parameters. These platforms are established process development tools and allow parallel, automated, and standardized workflows. Scale down devices (SDDs) operated in a HTS regime accelerate process development efforts and workflow at reduced material consumption.[3–6] Beside model-assisted scale transfer publications,[2,6–9] investigations of HTS are usually limited to batch isotherm determination and/or K_P screenings. In addition, studies on HTS membrane chromatography applications are rarely found when compared with resin-based HTS applications. These limitations have been addressed earlier.[10] However, optimal process development, scale up, and novel process designs depend on the limitation of the screening method used.

Displacement chromatography add a dedicated displacer that compete with at least one component and induce a partial elution and thus separation of the stationary phase bound components. In the case that the feed mixture itself exhibit competitive binding components and the product is displaced from the stationary phase by the impurities, a typical frontal chromatography (FC) mode is used.[11,12] The presented overload bind and elute (OBE) now follows the same principle as FC but consist of product binding and an additional elution step. Both process modes, FC and OBE mode, apply higher mass loading beyond the dynamic breakthrough concentration.[13–15] Consequently, the application of components with similar binding properties and thus competitive adsorption based in displacement effects occur. Thereby, FC and OBE overloading the stationary phase and thus increases its utilization and productivity.[12,14–16]

In the light of the above, given typical multicomponent process streams competitive adsorption-based displacement effects can only be considered for process development if the screening method identifies those. Especially in separation tasks with closely similar molecules as monomer and aggregates such as higher molecular weight species (HMWS), OBE chromatography offers the advantage of an increased productivity avoiding the implementation of narrow cut points or extended gradients (i.e., pH value, conductivity [CD]) leading to product dilution.

For monoclonal antibodies (mAbs), aggregates in the final formulation pose a risk due to various influences on the activity and stability of the product.[17,18] In the established platform process for the purification of mAbs, the typical Protein A capture step is followed by one or two additional chromatographic purification steps.[19,20] High purity of active pharmaceutical ingredients are obtained by separating HCP, DNA, leached Protein A, viruses, and HMWS aggregates in these chromatography steps. For the separation of mAbs and their HMWS,

cation and hydrophobic interaction chromatography are established methods.[19–21] In addition, ceramic hydroxyapatite and mixed mode[21,22] chromatographies are also used for the removal of aggregates.[19] The different chromatographic types for the reduction of HMWS can be applied in bind and elute, flow through, weak partitioning chromatography, FC, or OBE.[15,19,20,23,24] When separating HMWS with a chromatographic mode that contains high salt concentration or varying pH values, the risk of new aggregate/HMWS formation during the step is highly probable.[17,18] Given the widely constant conditions, OBE chromatography offers the advantage of a stationary state with regard to salt load and pH value and should thus suppress new aggregate formation. The significant advantages of membrane adsorber (MA) over resin-based chromatographic processes when used for contaminant removal in FT mode[25,26] underline their application for OBE chromatography. In addition, the high mass transfer rates observed in MAs furthermore promote competitive binding-based displacement effects and maintain the typically high productivity. During the last decades, several efforts in research and process development were carried out investigating competitive-based displacement effects and their use.[14–16,23,24,27–31] However, currently no screening strategy exists to investigate potential displacement effects applying membrane chromatography on a robotic screening platform.

In this paper, we introduce a process development strategy for the determination of competitive binding-based displacement effects in mAb aggregate removal. Initially, principles behind competitive binding-based displacement effects are investigated and verified by mechanistic modelling of two different two-component mixtures. Subsequently, a new robotic HTS screening procedure is developed and evaluated in the light of a novel process design. The newly developed robotic HTS screening procedure is applied for aggregate removal process development when processing mAbs. To illustrate its applicability towards process development using OBE chromatography, a Sartobind® S a cation exchange (CEX) MA is investigated. Specifically, during the HTS OBE mode, the CEX MA is loaded until saturation, washed, and partially eluted in repeating cycles at stepwise increased salt concentrations. In addition, the method can be used to identify the potential presence of competitive binding-based displacement effects and predict the optimum process condition. The process parameter and displacement effects are confirmed with benchtop recycle experiments. In the recycling experiments, at least 60 times loading volume was passed twice over a Sartobind S MA and the displacement effects were analyzed with size-exclusion chromatography (SEC) in the breakthrough. Finally, this processing mode is shown to elevate yield and enhance selectivity when

comparing with a classical FT mode, which is typically stopped at a HMWS product content below 1%.

2 | MATERIALS AND METHODS

2.1 | Materials

The applicationsfor material used in this work can be divided into (a) HTS and benchtop chromatographic experiments, (b) benchtop recycle experiments, (c) analytics, and (d) data handling, automation, and mechanistic modeling.

a) HTS and benchtop chromatographic experiments

The HTS is carried out with the HTS robot Lissy® 2002 GXXL/8P from Zinsser Analytic. FT and OBE chromatography experiments were performed using Äkta Prime™ and Äkta™ Explorer from Cytiva. The used MA devices were prototype setups, based on three flat sheet-stacked MAs with a diameter of 2.9 cm in a plastic housing, resulting in a liquid accessible diameter of 2.7 cm for the then 0.025 ± 0.003 cm bed height and 0.43 ± 0.05 cmş. Cellstar® 12-wellplates from Greiner Bio-one International GmbH were used for the fractionation of the SDD-HTS. The buffer preparation is done by dissolving the buffer salts in purified water, which is provided by an Arium® Water Purification System from Sartorius Stedim GmbH. The used salts were weighed with Sartorius Master^{pro} LP 12000S balance or Sartorius Expert LE225D-OCE from Sartorius Stedim Biotech GmbH with the components: sodium chloride (NaCl), hydrochloric acid (HCl), glycine, sodium acetate (NaAc), acetic acid, di-potassium hydrogen phosphate, potassium dihydrogen phosphate, disodium hydrogen phosphate di-hydrate, and sodium di-hydrogen phosphate di-hydrate from Carl Roth, trisodium citrate di-hydrate and acetone from VWR chemicals, citric acid monohydrate from Alfa Aesar, and ethanol from Sigma–Aldrich. For pH value adjustment, sodium hydroxide (NaOH) or HCl were used. Each buffer and load solution is prefiltered with a $0.45\,\mu m$ Sartopure® and a $0.2\,\mu m$ Sartolab® RF vacuum filter from Sartorius Stedim Biotech GmbH. The CHO-fermented mAb is a Sartorius Stedim Biotech GmbH internal load solution. Further purification was done with a MabSelect™ Sure™ lab column (5 cm diameter, 192 ml volume) provided by Cytiva and an Äkta Prime™ system. The eluate contained approximately 18 g/L mAb and a mAb aggregate level of approximately 0.5–2%. Enrichment of the aggregate content of the clarified mAb solution to 2–8 % is done with a pH shift. Aggregation with a temporary pH shift is a commonly used method for aggregation.[18,32,33] After diluting the 0.1 M pH

~3 glycine-buffered mAb solution three times with KPi buffer, the pH value is adjusted to pH 3 with 0.5 M HCl or 0.5 M H_3PO_4. The aggregation time was set to 2 h with stirring at 150 rpm. Finally, the pH is readjusted to pH 7 with 0.5 M NaOH. Following this, the respective aggregated mAb solution is again purified with the protein A column fractionated in a prefraction, high concentration, and postfraction. The prefraction and postfractions of all chromatographic runs are pooled, and pH adjusted again loaded to the protein A column, resulting in pooled high concentration fraction solutions that exhibit mAb concentrations of up to 22 g/L. The final load solutions were prepared by diluting the high concentrated aggregated mAb solution with the respective buffer, with a minimum dilution ratio of one to three. Each dilution buffer at each pH value was prepared with 0 and 1 mol/L NaCl to achieve appropriate salt concentrations. The pH value and CD was adjusted by mixing the solution with the respective buffer followed by an incubation period of one hour at room temperature. In a pH range of 5–7, the feed solution was diluted to 1–6 g/L with 0–0.3 M NaCl concentration. The used load and buffer stock solution for the HTS screening are NaAc (pH range 5–5.5) and potassium phosphate (pH range 6–7).

b) Benchtop recycle experiments

The benchtop OBE chromatography experiments in recycle mode were carried out with a mAb solution of 2–6 g/L monomer and 2–8% HMWS in 20 mM NaAc buffer at pH 5 or 5.5 and a NaCl-adjusted CD of 10 and 18 mS/cm, respectively. The benchtop experiments were conducted applying a MA in a silicon housing stabilized with a plastic jacket with 20 or 40 stacked flat sheet Sartobind® S membranes resulting in a bed volume of 4.6 ± 0.2 and 8.4 ± 0.3 ml, respectively.

c) Analytics

Overall protein concentration was measured at 280 nm wavelength with a VivaSpec® UV reader from Sartorius Stedim Biotech GmbH. The IgG and its HMWS concentration were measured with a Yarra™ 3 μm SEC 3000 column of 300 × 7.8 mm from Phenomenex using Dionex™ UltiMate™ 3000 HPLC System from Thermo Scientific™ at a flow rate of 1 ml/min.

d) Data handling, automation, and mechanistic modeling

The HTS method automation was done with WinLissy (version 7) from Zinsser Analytic. UNICORN® from Cytiva was used for FT experiment recipe writing. The IgG and its HMWS concentration were quantified with

the Chromeleon™ 6.80 from Dionex. Experimental results evaluation and chromatographic data analysis were done with Origin® 2018b from OriginLab Corporation. Mechanistic modeling was done with ChromX™ provided by GoSilico GmbH.

3 | METHODS

A full list of abbreviations, symbols, and indexes used throughout this work is presented at the end of this manuscript.

3.1 | SDD: experimental setup

Each SDD contains a membrane bed consisting of three flat sheet membrane discs with 27 mm diameter and 240–280 μm thickness resulting in a bed volume of 0.41–0.48 ml, respectively, as illustrated in Figure 1(A). A Sartobind® S membrane with a mean pore diameter of 3–5 μm and a ligand density of 2–5 μeq/cmš is used in this work. Each SDD exhibits a septum port, through which a robotic needle can penetrate to inject solution with a positive pressure into the device. To test and assess the targeted average pipetted volume accuracy of less than ±3 % for an injection velocity of 500 μl/s, a volume calibration routine to reduce the deviation between set and measured dispensed volume was established using 200, 400, 800, 1500, 2500, and 4000 μl water in triplicate for each needle prior to each experiment. In case the targeted accuracy could not be reached, the volume correction factors of the robotic system are adjusted in the HTS robotic software. The HTS setup comprises eight SDDs fixed on a holder plate to be operated in a parallel fashion, see Figure 1(B). Below the SDD holder plate, four movable 12-well plates collect the fractions of the eight devices where each well can hold a maximum of 5 ml solution and complete the SDD-HTS.

3.2 | Competitive adsorption-based displacement: delta interaction strength

Displacement effects have been exhaustively investigated by several researcher as for example, the Steven Cramer group,[23,34–36] among others as Georges Guichon group[37–39] and Massimo Morbidelli group.[12,40,41] In displacement chromatography, components of a mixture, which is bound to the stationary phase, are selectively eluted by applying specific displacer. Selection and characterization of a possible displacer can be achieved calculating the separation factor α in Equation (1) based on the dynamic affinities λ

calculated in Equation (2) derived by the steric mass action (SMA) isotherm model in Equation (3).

$$\alpha = \frac{\lambda_i}{\lambda_j} \tag{1}$$

$$\lambda_i = \left(\frac{K_i}{\frac{q_{\text{Displacer}}}{c_{\text{Displacer}}}} \right)^{\frac{1}{\nu_i}} \tag{2}$$

$$c_{\text{eq},i} = \frac{q_i}{K_{\text{eq},i}} \cdot \left(\frac{c_S}{\Lambda - \sum_{j=1}^{n} (\sigma_j + \nu_j) \cdot q_j} \right)^{\nu_i} \tag{3}$$

Previous work of Cramer and coworkers is adapted for the identification of competitive binding-based displacement effect during the presented OBE chromatography mode. Rearrangement of Equation (3) leads to the identification of three groups as displayed in Equation (4). T1 ligand availability for the component m, T2 reduction of available ligands by the bound component i, and T3 competitive adsorption depending on surface charge, sum of steric hinderance σ, and characteristic charge ν of each component. Following this, the interaction strength and thus competitive binding-based displacement rely on the bound components and the applied liquid concentration when compared to Equation (3).

$$q_m = \underbrace{\frac{\Lambda}{(\nu_m + \sigma_m)}}_{T1} - \underbrace{\frac{q_i^{\frac{1}{\nu_i}} \cdot c_s}{(c_{\text{eq},i} \cdot K_{\text{eq},i})^{\frac{1}{\nu_i}} \cdot (\nu_m + \sigma_m)}}_{T2}$$
$$- \underbrace{\frac{\sum_{j=2}^{n} (\nu_j + \sigma_j) \cdot q_j}{(\nu_m + \sigma_m)}}_{T3} \tag{4}$$

The identification of competitive adsorption-based displacement effects can be conducted by reducing Equation (4) for a two-component system in Equation (5). This said, the salt molecule is not considered as a component in this case, which would be needed for an analytically correct correlation.

$$q_1 = \underbrace{\frac{\Lambda}{(\nu_1 + \sigma_1)}}_{T1} - \underbrace{\frac{q_2^{\frac{1}{\nu_2}} \cdot c_s}{(c_{\text{eq},2} \cdot K_{\text{eq},2})^{\frac{1}{\nu_2}} \cdot (\nu_1 + \sigma_1)}}_{T2} - \underbrace{\frac{(\nu_2 + \sigma_2)}{(\nu_1 + \sigma_1)}}_{T3} \cdot q_2 \tag{5}$$
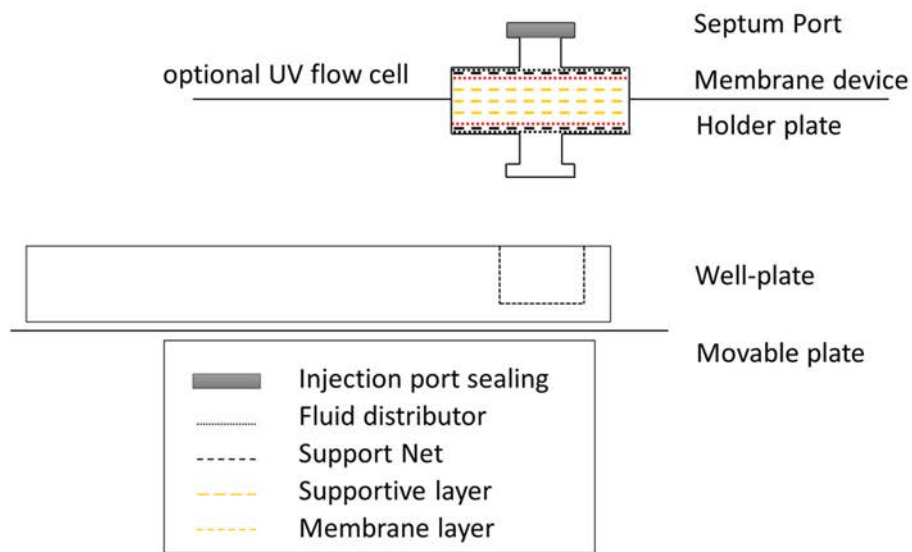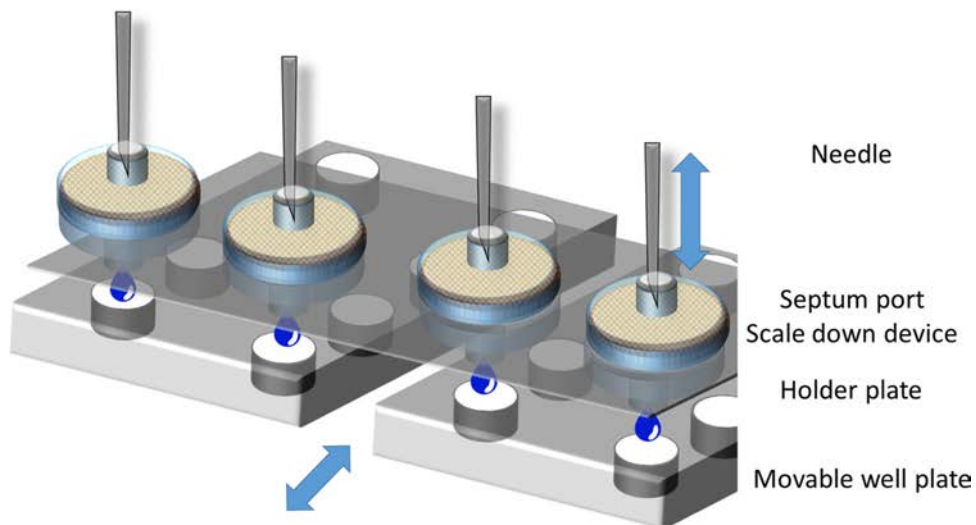
FIGURE 1 (A) SDD setup in which the liquid passes a fluid distributor followed by a support net and the three membrane layers, (B) SDD-HTS setup: needle injects the liquid through the septum port into the SDD, which is fixed to a holder plate. The holder plate holds eight membrane devices. Four movable well plates are used for the fractionation while each well plate collects the fraction for two membrane devices

However, in Equation (5), the two terms T2 and T3 can have an impact on displacement effects. Based on the parameters given, T3 specifies the steric and charged-based differences between the components and thus be used for the displacement identification. The two-component interaction strength increases with the difference between the components. Following this, with a high interaction strength, component 1 will be displaced by component 2. Therefore, T3 is defined as delta interaction strength in Equation (6).

$$\text{Delta interaction strength} = \frac{(\nu_2 + \sigma_2)}{(\nu_1 + \sigma_1)} \qquad (6)$$

	Unit	Ribonuclease A	Cytochrome *c*	IgG	IgG HMWS
Feed concentration	M	1.3e−04	8.0e−06	1.2e−05	3.3e−07
Kinetic	s(M)^y	0.013	0.013	0.013	0.066
Equilibrium	–	0.148	0.307	9.91	14.4
Charge	–	5.11	5	4.4	4.93
Steric	–	28.88	28.7	513.8	12,915.5
Ionic capacity	M	0.8	0.8	0.5	0.5

TABLE 2 OBE screening procedure

Step (–)	Step size (ml)	Total volume (ml)	Conductivity (CD) (mS/cm)
L1	2–4	28	10
W1	2–4	10–12	10
E1	4	8	20
L2	2–4	14	20
W2	2–4	10–12	20
E2	4	8	30
L3	2–4	14	30
W3	2–4	10–12	30
E3	4	8	40

3.3 | Mechanistic model analysis

To validate the above deduction, the outcome of two case studies based on the separation of ribonuclease A and cytochrome C as well as IgG monomer and its HMWS is examined. The differences between BE and OBE chromatography mode are evaluated by a detailed equilibrium-dispersive mechanistic model analysis applying an SMA isotherm, each by means of locally resolved stationary interaction, column profile and isothermal behavior. The investigated stationary phase for both scenarios is a MA of 8.34 ml, a porosity of 0.75 and a bed height of 13.75 mm. The respective fluid dynamics of the system and MA were characterized with a step function acetone tracer experiment. The ionic capacity for the used Sartobind® S was determined by titration of the module using an Äkta™ Explorer. The used flow rate was 14 ml/min. In Table 1, the competent parameters are listed for ribonuclease A and cytochrome *c* obtained from Osberghaus et al.[8] The kinetics were assumed to be equal and comparable to IgG. The IgG and HMWS SMA isotherm parameters were assessed using the HTS BE results published earlier[10] (results not shown here).

3.4 | HTS$_{OBE}$

The developed screening procedure leading to the application of OBE chromatography suitable for classical process range determination and difficult to assess and/or identify effects such as displacement. The procedure can be described by a repeated BE mode with partial elution. The HTS$_{OBE}$ procedure and the resulting chromatograms are depicted in Table 2 and Figure 2.

In contrast to the HTS$_{BE}$ mode discussed earlier,[10] the equilibrated MA is purposely overloaded by adding a load mass of twice the by estimated static binding capacity (prior knowledge), here in 2–4 ml steps up to 28 ml load (L1). Subsequently, the MA is washed with 10–12 ml in 2–4 ml steps (W1) and partially eluted with 8 ml in 4 ml steps (E1) with one CD step. This is followed by loading the MA (L2) containing 14 ml load in 2–4 ml steps with the same conditions as the elution step (E1) before. After the anew loading, the procedure is repeated. The approach is completed with an 8 ml regeneration and 12 ml reequilibration storage step in 4 ml steps. Liquid dispensing velocity was set to 500 μl/s. The loading concentration for each pH and CD value is listed in Table 3. Every pipetting step

	Loading concentration					
	CD 10 (mS/cm)		CD 20 (mS/cm)		CD 30 (mS/cm)	
pH	IgG monomer	HMWS	IgG monomer	HMWS	IgG monomer	HMWS
5.0	4.92	0.16	4.84	0.15	3.89	0.11
5.5	5.65	0.16	5.01	0.20	4.80	0.17
6.0	5.03	0.15	5.11	0.16	3.83	0.15
6.5	5.36	0.20	5.30	0.19	4.92	0.16
7.0	5.34	0.24	5.07	0.21	4.94	0.20
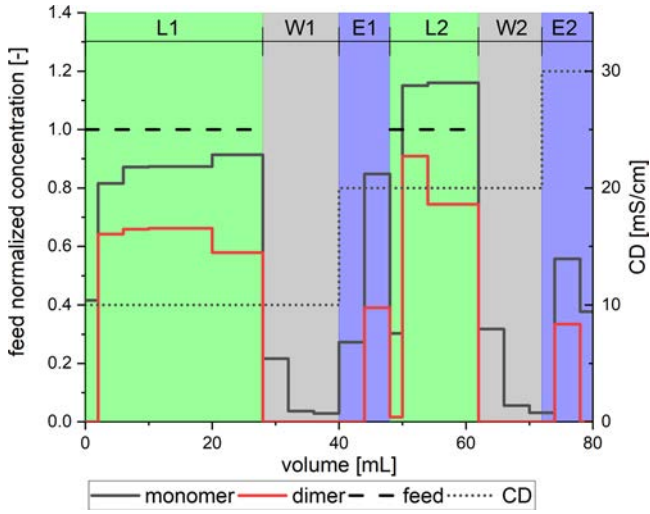
FIGURE 2 Exemplary OBE mode with two phases of a BE mode as loading phases L1, L2 (green areas), wash phases W1, W2 (gray areas) and elution phases E1, E2 (blue areas). The OBE mode comprises a sequence of load (L), wash (W), and elution (E) steps. The parameters used are listed in Tables 2 and 3. If a component concentration exceeds its loading concentration in the loading step while the other component concentration remains below, its loading concentration displacement effects are identified

3.4.1 | Binding capacity

An outcome of the HTS_{OBE} results are static binding capacities for process maps. HTS_{BE} and HTS_{OBE} will lead to the same static binding capacity if no displacement effects are present. If displacement effects are present, the dependency of the static binding capacity with the loaded mass will lead to differences in the static binding capacity between the HTS_{BE} and HTS_{OBE}. The static binding capacity at the initial CD at a given pH value is calculated using Equation (7). In Equation (7), the sum difference of each component loaded mass and flow through fraction mass equals the static binding capacity, respectively.

$$q_{\text{FT MaxLoad},i} = \frac{1}{V_{\text{MA}}} \cdot \left(\sum_{k=1}^{l} \sum_{i=1}^{n} c_{\text{FT Load},i,k} \cdot V_{\text{FT Load},k} \right.$$
$$\left. - \sum_{k=1}^{l} \sum_{i=1}^{n} c_{FT\,i,k} \cdot V_{FT,k} \right) \tag{7}$$

3.4.2 | Identification of competitive adsorption-based displacement

Raw data obtained by a HTS_{OBE} procedure are analysed by means of a term named displacement identifier (DI). In Equation (8), each component concentration c_i is normalized by the loading concentration $c_{\text{feed},i}$. The normalization thus allows to highlight two distinct situations: (1) the normalized component concentration is bigger than one and thus indicates displacement; (2) the normalized component concentration of the component is below one and thus indicates the action of a competitive higher attracted molecule. With this in mind, the DI in Equation (9) is the product of each normalized concentration reduced by one and is considered when the Phase k is equal to load phase as well as the absolute deviation to the step before is less than 10%. Consequently, a DI below zero indicates displacement effects and a DI equal or higher than zero indicates no competitive adsorption-based

eluate is collected in a cavity of a movable well plate and analyzed by SEC. Based on prior knowledge, the CD was set to observe a high, medium, and low binding capacity range. For unknown binding conditions of a stationary phase, the CD range might be extended, and/or smaller CD steps could be used.

Limitations of the HTS_{OBE} mode: In the presence of competitive adsorption displacement effects, the static binding capacity may not be determined with absolute certainty, based on the unknown loading duration needed. However, the HTS_{OBE} mode for displacement effect evaluation is capable to identified competitive adsorption, thereby increasing contaminant binding capacity, optimal process conditions enhancing utilization and recovery.
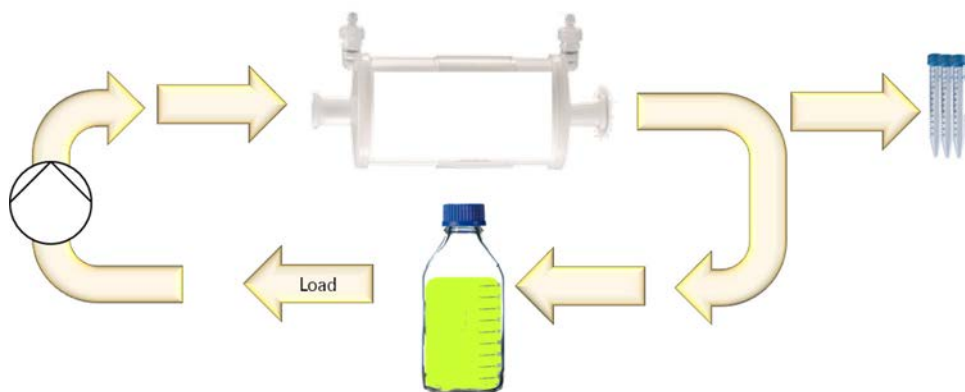
FIGURE 3 Schematic recycling experiments, the load is pumped from the loading vessel over the MA and recycled in the loading vessel. Fractions are analyzed via SEC

displacement. Applying the DI for competitive adsorption-based displacement effect analysis in HTS_{OBE} loading phase requires a stationary phase saturation of at least one component.

$$c_{\text{Norm},i,k} = \frac{c_i}{c_{\text{feed},i}} \tag{8}$$

$$\text{DI}_k = \left(c_{\text{Norm},i,k} - 1\right) \cdot \left(c_{\text{Norm},i+1,k} - 1\right)\Big|_{=\text{Load} \wedge \text{ABS}\left(\frac{\partial c}{\partial V}\right) \leq 10\,\%} \tag{9}$$

3.5 | Scale up

For a scale-up validation of the HTS_{OBE} data shown in Figure 3, benchtop experiments were conducted as follows. Initially, a 4.6 ml prototype Sartobind® S was used with a volume of 500 ml recycled twice over the MA. In addition, a 8.2 ml device was used for recycle and a single FT experiment. The equilibrated MA is loaded and the flow through fractionated into 5 ml samples until reaching a total of 10 membrane volumes (MV). Following this, each 100 ml, a 5–10 ml sample was collected. All samples were analyzed by SEC. If not sampled, the liquid is recycled into the storage tank. In the recycling experiments, feedstock solutions of 1.8–3.4 g/L IgG monomer, 0.2–0.96 g/L dimer, and 0–0.04 g/L IgG oligomer were loaded at pH 5 and 5.5 and CDs of 10, 11, and 18 mS/cm. A mass balance is used to determine the concentration in eluate and stirred tank. To do so, load is weighed at the beginning and at the end of the experiment; the states in between were calculated with the taken SEC samples.

4 | RESULTS AND DISCUSSION

4.1 | Mechanistic process understanding

Addressing the standardized biopharmaceutical mAb process with its protein A purification step and typically small levels of impurities, both subsequent purification strategies—BE and/or MA FT mode—are currently used.

The typical challenge in a mAb platform process is the separation of the target molecule (IgG) showing a higher feed concentration but lower charge/affinity to CEX ligands (component 1) and an impurity (i.e., aggregates) showing a low feed concentration but usually higher charge/affinity to CEX ligands (component 2). Based on the highlighted correlations between SMA parameters and possible displacement identification (Equation 4), the introduced interaction strength (Equation 6) is initially used for a theoretical assessment.

Competitive adsorption-based displacement effects occur now when the difference/delta between these surface-charge related affinities increases. A schematic illustration of these effects at BE and OBE chromatography modes is shown in Figure 4. Initially, the higher concentrated molecule (component 1, mAb) will occupy the available surface of the stationary phase, but upon further loading will—in the case displacement takes place—eventually be displaced by the lower concentrated impurity (component 2, aggregate). In a BE mode, potential displacement effects are hardly seen during load and elution. This said, displacement effects will change the internal "column profile" independent of process mode. In OBE chromatography, potential displacement effects, however, can be exploited to increase utilization of the
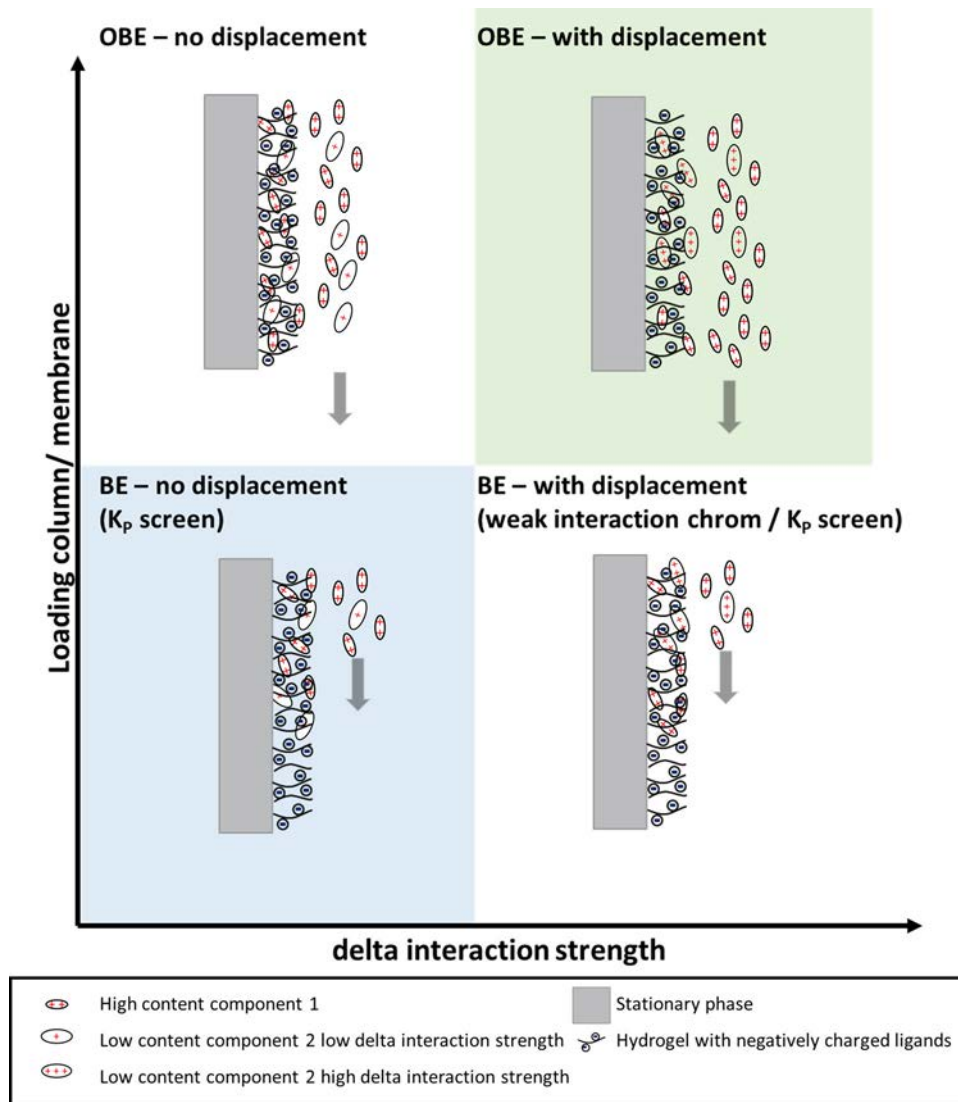
FIGURE 4 Schematic illustrations of the molecular processes along the stationary phase length. The process mode is a function of column load; FT mode for high column load and BE mode for low column load. Displacement effects between two components are governed by the delta interaction strength

stationary phase and feedstock purity. Thus, the column/membrane load determines the process mode—BE or OBE—whereas the delta interaction strength determines molecular processes determining the occurrence and strength of displacement effects.

The above presented Figure 4 is validated by the two presented mechanistic model-based analysis of two high load FT mode simulation using isotherm data from ribonuclease A and cytochrome c as well as IgG monomer and its HMWS (see Table 1) in Figure 5. The separation of ribonuclease A and cytochrome c with a delta interaction strength of 0.99 shows no significant displacement effects, whereas IgG monomer and its HMWS with a delta interaction strength of 25 clearly show displacement effects.

Figure 5(A) reviews the resulting process signals in terms of obtained chromatograms and Figure 5(B) highlights the respective isotherms behind this behavior. Assessing the obtained chromatograms in a BE mode it becomes clear that displacement behavior will only lead to a shift in retention time and slight changes in the shape of the elution peak. The delta interaction strength is only visible in the distance of the resulting peaks as a function of elution conditions. For FT mode, where the stationary phase is overloaded with process feedstock potential disassembly becomes visible during load showing a higher c_{out} than c_{in} of component 1.

Although the actual affinity of a component (either single or in a mixture) remains widely unchanged (Figure 5(B(1))), the most prominent difference when assessing
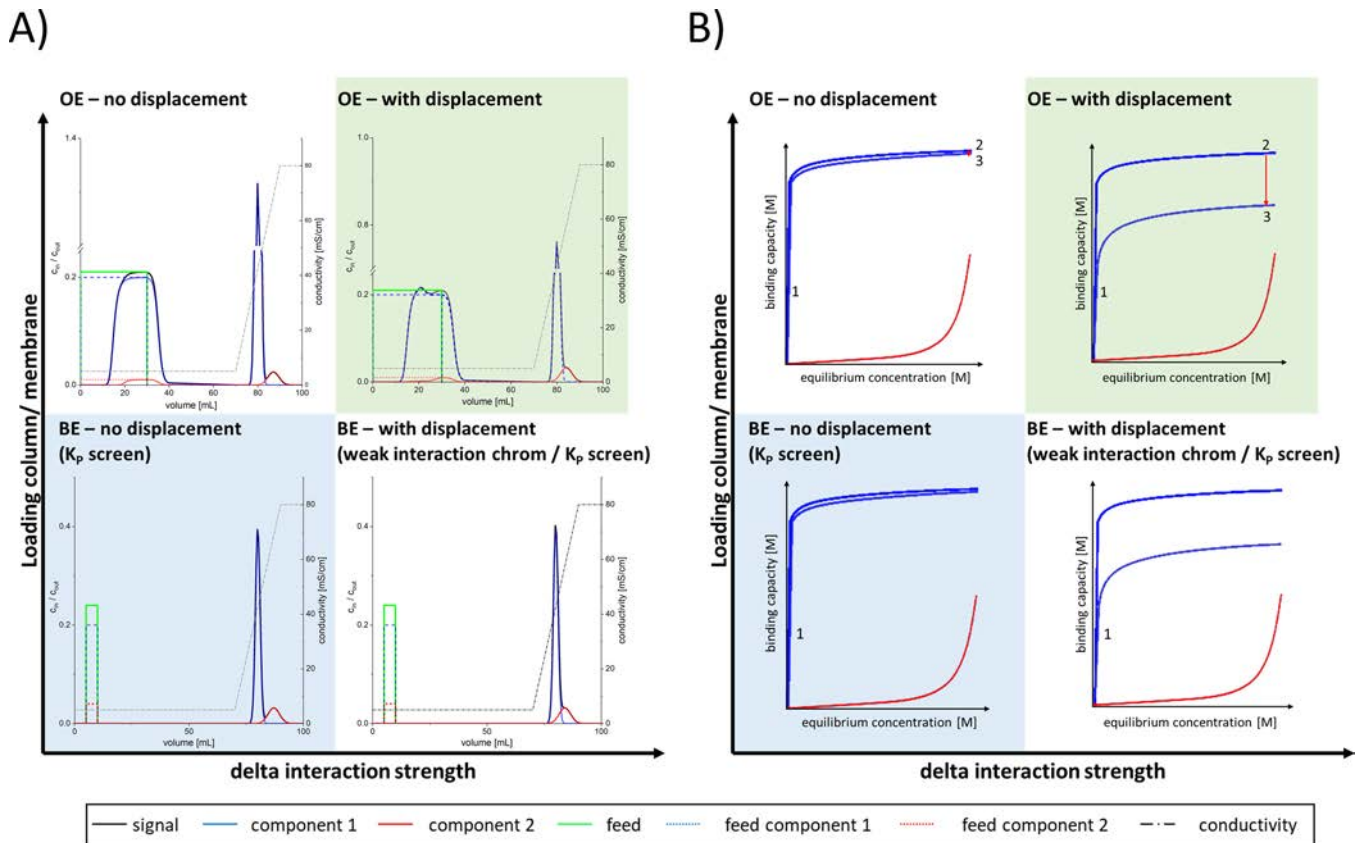
FIGURE 5 Visualization of the obtained process signal in terms of chromatograms (A) and the respective isotherm shapes (B). The signals are sorted compared with the schematic description in Figure 4 highlighting the process mode—BE or FT—being a function of column saturation and the underlying molecular processes being a function of the delta interaction strength. The most prominent indicator for displacement effects is clearly seen in the load behavior under FT conditions

the isotherms behind the adsorption behavior is the reduction in binding capacity of component 1 when transitioning from a single component systems to a two component mixture (Figure 5(B(2,3))).

The loading phase of ribonuclease A and cytochrome *c* is dominated by the ligand saturation through ribonuclease A being higher concentrated and exhibiting a higher affinity to the stationary phase. Cytochrome *c* binds to the stationary phase as expected by its smaller concentration value, but reduces the static binding capacity of ribonuclease A insignificantly with a 5% decrease at the cytochrome *c* breakthrough. During further loading, the ribonuclease A liquid concentration strives towards its feed concentration, while no displacement effects could be observed.

For IgG monomer and its HMWS, displacement effects can be assumed solely based on the delta interaction strength. The displacement effects are then observed during the loading phase when the IgG monomer concentration exceeds its feed concentration. This effect was described previously[10] and is confirmed with the monomer binding capacity reduction by the HMWS concentration breakthrough. The HMWS concentration breakthrough

indicates an HMWS-saturated phase. The relative IgG binding capacity decreases with over 40% when the HMWS loading content increases from 1% to 2%.

In summary, displacement effects are present if the delta interaction strength is greater than one and thus the process concentration of component 1 exceeds its feed concentration in the loading phase. In addition, the concentration of the component with the higher affinity (component 2) will remain below its feed concentration during active displacement. As the most prominent indicator of displacement processes is found during the load step, a reliable screening procedure is introduced: the OBE mode. Although classical screening procedures[10] use several elution steps to determine the process range, displacement effects might be missed, this OBE mode investigates concentration behavior during load at several different salt concentrations.

Both, the HTS$_{BE}$ and HTS$_{OBE}$ modes result in the same static binding capacity under the following assumptions: identical loading composition and process conditions and no molecular effects such as displacement present. In this scenario, the OBE mode can also be used for
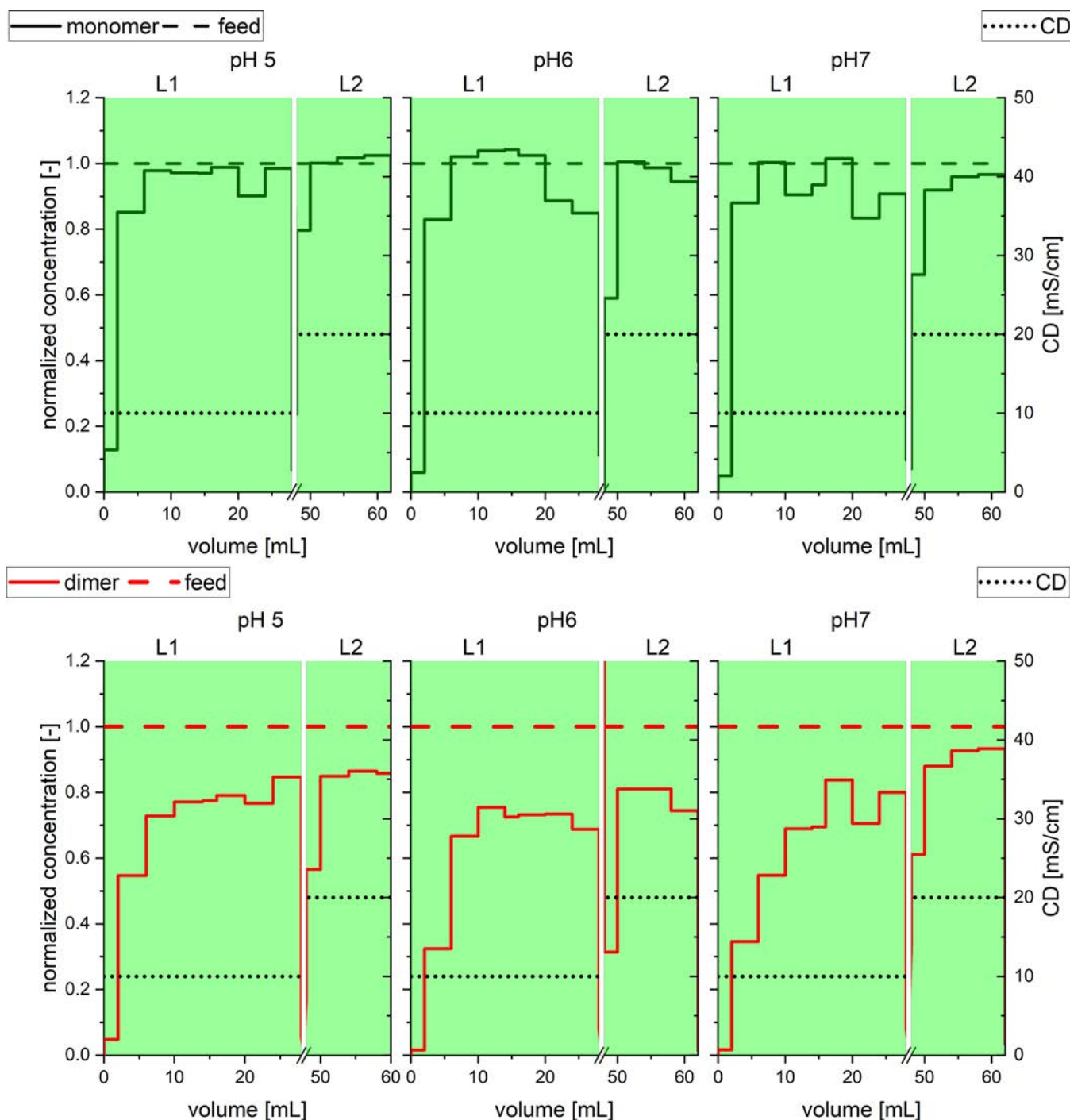
FIGURE 6 Concentration profile of load fraction under OBE mode of Sartobind® S IgG; (1) pH 5; (2) pH 6; (3) pH 7; IgG monomer (top row) and concentration IgG dimer (bottom row); the first loading step L1 is performed at low salt concentration, followed by a wash and stepwise increased salt concentration in the elution step E1. The next loading (L2) is performed at the same salt concentration as chosen for the elution and the procedure is continued as before

conventional process parameter determination. In contrast to the BE mode, the OBE mode offers the possibility to identify potential dynamic effects. The latter, however, to the cost of a lower economic use of resources during the screening procedure such as higher sample and buffer consumption.

4.2 | OBE mode

In Figure 6, the loading steps (L1, L2) of a Sartobind® S MA in a SDD-HTS setup applying the OBE mode at pH 5, 6, and 7 are shown. The CD values shown in Figure 6 were 10 mS/cm (L1) and 20 mS/cm (L2). All
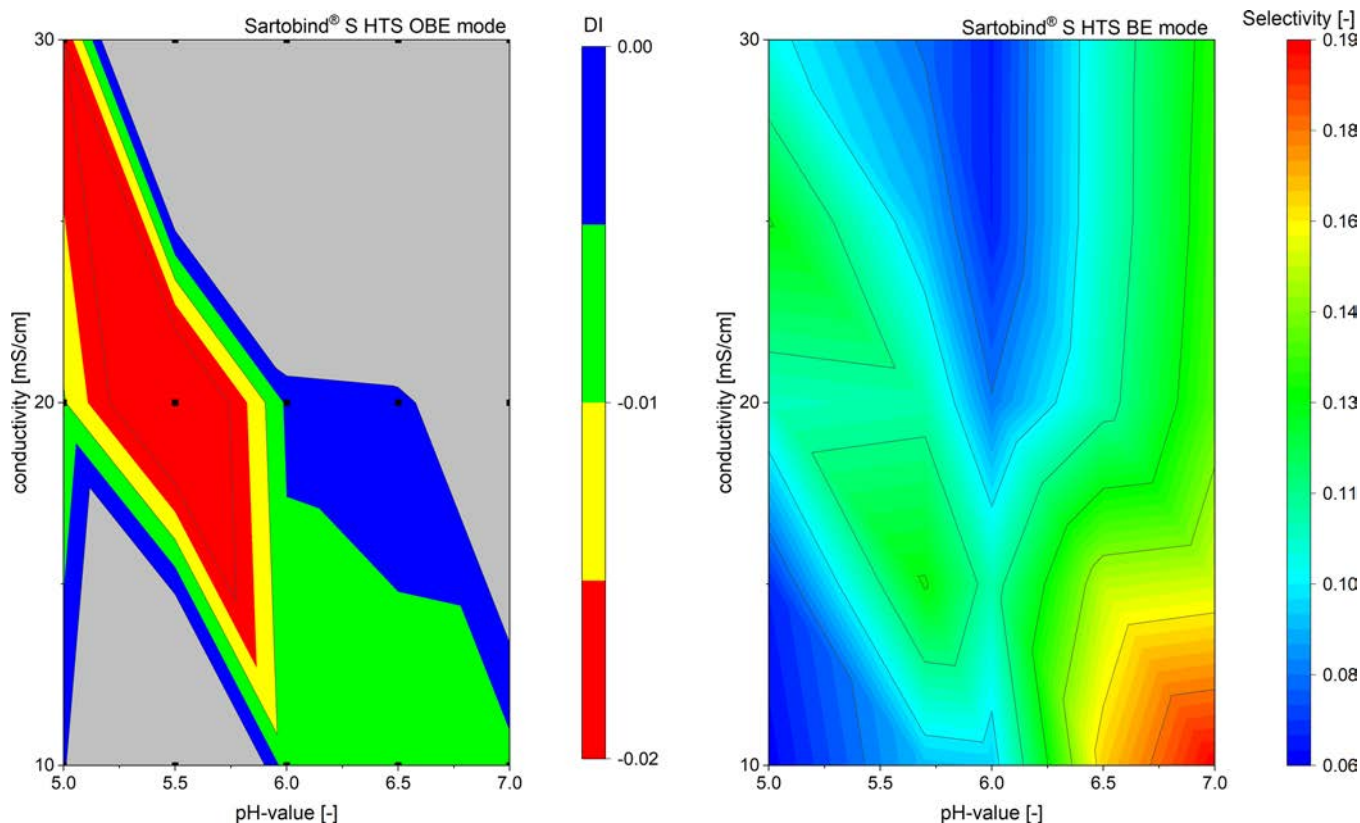
FIGURE 7 OBE DI map for Sartobind® S and IgG in comparison with BE selectivity map. The DI map shows with decreasing pH value and with the conductivity increasing displacement effects. The color code for displacement is: gray no displacement detected and increasing displacement effects determined from blue to green over yellow and red. To facilitate the comparison of the determined DI map, the selectivity map of IgG monomer and HMWS, determined in the HTS SDD BE mode published earlier by us,[7] is shown in the upper right corner. The applied BE and OBE mode show similarities in selectivity and D_i value, respectively

collected fractions are analyzed for monomer and HMWS content using off-line SEC. The MA ligand saturation is achieved in the first loading step L1. When examining L1 at pH value 5, the IgG monomer loading concentration is reached but not exceeded. In addition, the IgG dimer loading concentration is not reached, indicating potential displacement effects by competitive adsorption. However, deviation in the measurement and experimental work cannot be excluded and a clear statement is—for this scenario—not possible. In general, competitive adsorption-based displacement effects are only considered given that the behavior of both components indicates this. Considering the loading phase L2 at pH 5, it is observed that the monomer concentration exceeds the loading concentration, whereas the dimer concentration remains below its start/feed concentration. In this case, both components indicate a clear competitive adsorption induced displacement scenario. Based on the experimental quality for pH 7, valid statements are hardly possible, the concentration course in the first loading phase imply competitive adsorption here as well.

Even though not directly recognizable looking at the raw data presented in Figure 6, applying the OBE leads to an assessment of displacement effects applying a DI map. Figure 7 shows the obtained DI values of the screening data presented in Figure 6. A DI below 0 displays potential displacement effects. The lowest DI obtained from the different loading fractions is applied for the DI map. Doing so, a DI of −0.01 and −0.027 represents for example an excess of fraction concentration of the IgG over loading concentration of 5% and 10%, respectively. For Sartobind® S, IgG displacement effects increase with the salt concentration at decreasing pH value. At neutral to basic pH conditions, no displacement effects are observed. Displacement showed to be a fine interplay between surface charge (distance to isoelectric point of the components) and salt concentration (shielding of electrostatic interactions). The slight differences in DI show the difficulty to determine displacement effects. Decreasing binding capacity also decreases the concentration change of the lower attracted component, leading to detection limitations.

However, as displacement is a function of different interaction strength and thus the ability to separate two
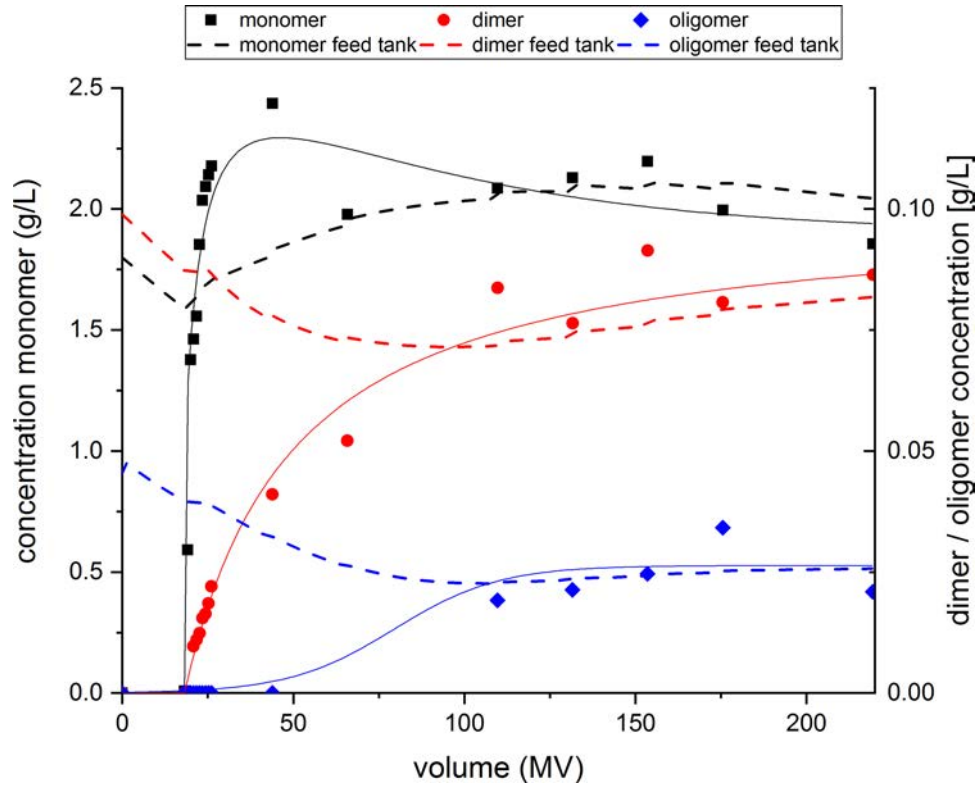
FIGURE 8 Simplified recycle experiment concentration profile at pH 5.5, CD 18 mS/cm. The IgG monomer increases the loading concentration and convergence then the loading concentration. In the range of 20–75 MV, the dimer and HMWS concentration do not reach the loading concentration that conform the displacement of IgG monomer

components in BE mode, it is not surprising that the DI course obtained for the OBE mode is comparable with the BE Sartobind® S selectivity band with increasing CD and decreasing pH value showed earlier.[10] In addition, Vogg et al.[12] have discovered similar process parameters in their investigations of displacement effects on Sartobind® S for a 50 kDa smaller antibody and its aggregate. In additional studies, applying the BE mode for pH 5.5 and 20 mS/cm showed binding capacities of 10 and 1 mg/ml for a IgG and its HMWS, respectively. Applying the OBE mode for the same conditions resulted in binding capacities of 10 mg/ml IgG and 3 mg/ml HMWS, respectively. In process development, this would result in a three-time higher load volume. This said, a higher loading volume at reduced IgG product binding enhances yield and productivity when compared with a classical FT approach. Accordingly, the OBE mode is centered between the BE mode facilitating for complex purification/feed impurity variability and the FT mode with high recovery/productivity.

4.3 | OBE recycle chromatography: case study

The OBE results obtained in the HTS setup were confirmed in an benchtop case studies expressing approximately

scale-up factors of 10 and 20. Five hundred milliliters of feed stock—containing 1.78 g/L IgG monomer, 0.96 g/L dimer, and 0.04 g/L IgG HMWS—were loaded/recycled two times on a 4.6 ml Sartobind® S device at pH 5 and CD 11 mS/cm (L1), pH 5.5 and CD 10 mS/cm (L2), also pH 5.5 and CD 18 mS/cm (L3). Additional experiments were conducted with an 8.4 ml device at pH 5 and CD 11 mS/cm (L1), pH 5.5 and CD 11 mS/cm (L2), also pH 5.5 and 18 mS/cm (L3). Figure 8 shows the recycle experiment obtained for the 4.6 ml Sartobind® S device at a pH 5.5 and CD 18 mS/cm (L3). The monomer concentration exceeds the loading concentration shortly after the breakthrough started. As a result of the fractionation, the load/vessel concentration decreases with the experimental period not only during adsorption, but also when mass is removed. Shortly after (1–2 MV) the IgG monomer, the IgG dimer breakthrough can be determined. The IgG dimer breakthrough is shallower than that of the IgG monomer. This characteristic can be caused by either strongly deviating isothermal parameters or different adsorption kinetic properties. The start of HMWS breakthrough curve is only detected between 75 and 110 MV. However, comparing the loading concentration profile between the components shows similarities between IgG dimer and HMWS, indicating similarities between the respective components.

During the experimental course, the displacement of the IgG monomers decreases as a result of the dimer concentration approaching its loading/vessel concentration. Thereafter, the IgG dimer concentration increases slightly over its loading/vessel concentration, which may indicate displacement by IgG HMWS.

Based on the recycle experiments described above, the presence of displacement effects at the determined OBE conditions could be confirmed. Liu et al.[23] used a Poros™ 50HS resin in column chromatography and gained with 0.3 column volume per minute 36% less IgG monomer and 66% higher aggregate binding capacity. For MA processing, we achieved comparable results. Using displacement effects in MA processing leads up to 45% less monomer and 88% higher aggregate binding capacity compared with one-time loading.

Furthermore, the recycle experiment confirms the previous findings of HTS BE and HTS OBE mode at pH 5.5 and a CD of 20 mS/cm. The HTS BE mode determined 10 mg/ml IgG and 1 mg/ml HMWS binding capacity, whereas HTS OBE mode and recycle experiment showed capacities of 10 mg/ml IgG, 3 mg/ml HMWS and 14 mg/ml IgG, 3 g/L HMWS binding capacity. The slightly higher binding capacity of the IgG for the HTS OBE mode when comparing with the OBE benchtop experiments is probably due to a lower CD value (18 < 20 mS/cm) and an also lower aggregate concentration (5.2% < 5.7%).

5 | CONCLUSION

The applied process development approach targeting displacement effects from investigations on protein adsorption to process design was shown for an example of separating IgG monomer from its HMWS. Theoretical investigations based on SMA isotherm parameter evaluation allow a direct assessment of possible displacement effects in a two-component mixture resulting in the introduction of the delta interaction strength. Following this, the theoretical findings could be verified experimentally leading to a DI process map guiding process development at large scale. The conventional SDD-HTS approach in BE mode[7] has been extended with the OBE approach introduced in this work, allowing the determination of displacement effects. The SDD-HTS OBE approach can be described as a repeated BE mode with partial elution. The OBE approach has been applied to IgG aggregate removal with Sartobind® S and in addition to the successful displacement effect identification, the determination of classical process parameters for FC or OBE chromatography mode has been confirmed. As a result of the recycling experiment, the IgG monomer binding capacity was reduced by 45% and that of the IgG aggregates increased by 88%.

LIST OF SYMBOLS
The abbreviations, symbols, and indices used in this work are listed in Tables 4, 5, and 6.

TABLE 4 Abbreviations

Abbreviations	Meaning	Unit
BE	Bind and elute	–
CD	Conductivity	–
CEX	Cation exchange chromatography	–
DBC	dynamic breakthrough capacity	–
DI	Displacement identifier	–
E_k	Elution step k	–
FC	Frontal chromatography	–
FT	Flow through	–
HCP	Host cell protein	–
HMWS	Higher molecular weight species	–
HTS	High-throughput screening	–
IgG	Immunoglobulin G	–
LC	Liquid chromatography	–
L_k	Loading step k	–
MA	Membrane adsorber	–
mAb	Monoclonal antibody	–
MM	Mixed mode	–
MV	Membrane volume	–
OBE	Overload bind and elute	–
SDD	Scale down device	–
SEC	Size-exclusion chromatography	–
SMA	Steric mass action	–
W_k	Wash step k	–

TABLE 5 Symbol

Abbreviations	Meaning	Unit
c^*_i	Concentration of component i	g/L
c_{Feed}	Feed concentration	M
c_i	Concentration of component i	M
c_{Norm}	Feed normalized concentration	–
c_S	Salt concentration	M
DI	Displacement identifier	–
Delta interaction strength	Two component displacement quantifier interaction strength	–
K	Equilibrium constant	–
M	Molar mass	g/mol
MV	Membrane volume	MV
MV_0	Slope center in membrane volume	–
q	Binding capacity	M
$q_{\text{MaxLoad},i}$	Static binding capacity calculated by the difference between loaded and unbound mass	M
T1	Equation term 1	M
T2	Equation term 2	M
T3	Equation term 3	M
V	Volume	mL
α	Separation factor	–
λ	Dynamic affinity	–
Λ	Ionic capacity	–
ν	Characteristic charge	–
σ	Steric hinderance	–

TABLE 6 Indice

Abbreviations	Meaning	Unit
i	Component	–
BE	Bind and elute mode	–
Dimer	IgG dimer	–
HMWS	IgG HMWS	–
k	Fraction/dispensing step	–
m	Component	–
Monomer	IgG monomer	–
OBE	Overload bind and elute mode	–
Total	Total, overall value	–

CONFLICT OF INTEREST
The authors declare no conflict of interest.

REFERENCES

1. Jagschies G, Lindskog E, Łącki K, Galliher P. *Biopharmaceutical Processing*. Elsevier; 2018. https://www.elsevier.com/books/biopharmaceutical-processing/jagschies/978-0-08-100623-8.
2. Keller WR, Evans ST, Ferreira G, Robbins D, Cramer SM. Use of MiniColumns for linear isotherm parameter estimation and prediction of benchtop column performance. J Chromatogr A. 2015;1418:94-102. https://doi.org/10.1016/j.chroma.2015.09.038.
3. Kistler C, Pollard J, Ng LS, Streefland M. High-throughput bioprocess development. Genet Eng Biotechnol News. 2016;36(7):30-31. https://doi.org/10.1089/gen.36.07.15.
4. Bareither R, Bargh N, Oakeshott R, Watts K, Pollard D. Automated disposable small scale reactor for high throughput bioprocess development: a proof of concept study. Biotechnol Bioeng. 2013;110(12):3126-38. https://doi.org/10.1002/bit.24978.
5. Shukla AA, Rameez S, Wolfe LS, Oien N. *High-Throughput Process Development for Biopharmaceuticals*; 2017 //2018; 165. Springer, Cham. https://link.springer.com/chapter/10.1007/10_2017_20.
6. Wiendahl M, Schulze Wierling P, Nielsen J, Christensen DF, Krarup J, Staby A, et al. High throughput screening for the design and optimization of chromatographic processes – miniaturization, automation and parallelization of breakthrough and elution studies. Chem Eng Technol. 2008;31(6):893-903. https://doi.org/10.1002/ceat.200800167.
7. Keller WR, Evans ST, Ferreira G, Robbins D, Cramer SM. Understanding operational system differences for transfer of miniaturized chromatography column data using simulations. J Chromatogr A. 2017;1515:154-63. https://doi.org/10.1016/j.chroma.2017.07.091.
8. Osberghaus A, Hepbildikler S, Nath S, Haindl M, Lieres Ev, Hubbuch J. Determination of parameters for the steric mass action model–a comparison between two approaches. J Chromatogr A. 2012;1233:54-65. https://doi.org/10.1016/j.chroma.2012.02.004.
9. Benner SW, Welsh JP, Rauscher MA, Pollard JM. Prediction of lab and manufacturing scale chromatography performance using mini-columns and mechanistic modeling. J Chromatogr A. 2019;1593:54-62. https://doi.org/10.1016/j.chroma.2019.01.063.
10. Stein D, Thom V, Hubbuch J. High throughput screening setup of a scale-down device for membrane chromatography-aggregate removal of monoclonal antibodies. Biotechnol Prog. 2020:e3055. https://doi.org/10.1002/btpr.3055.
11. Stone MT, Cotoni KA, Stoner JL. Cation exchange frontal chromatography for the removal of monoclonal antibody aggregates. J Chromatogr A. 2019;1599:152-60. https://doi.org/10.1016/j.chroma.2019.04.020.
12. Vogg S, Pfeifer F, Ulmer N, Morbidelli M. Process intensification by frontal chromatography: performance comparison of resin and membrane adsorber for monovalent antibody aggregate removal. Biotechnol Bioeng. 2019. https://doi.org/10.1002/bit.27235.
13. Nadarajah D, Mehta A, Inventors; Genentech, Inc. Overload and elute chromatography. US20140301977.
14. Brown A, Bill J, Tully T, Radhamohan A, Dowd C. Overloading ion-exchange membranes as a purification step for monoclonal antibodies. Biotechnol Appl Biochem. 2010;56(2):59-70. https://doi.org/10.1042/BA20090369.

15. Ichihara T, Ito T, Kurisu Y, Galipeau K, Gillespie C. Integrated flow-through purification for therapeutic monoclonal antibodies processing. MAbs. 2018;10(2):325-34. https://doi.org/10.1080/19420862.2017.1417717.

16. Reck JM, Pabst TM, Hunter AK, Carta G. Separation of antibody monomer-dimer mixtures by frontal analysis. J Chromatogr A. 2017;1500:96-104. https://doi.org/10.1016/j.chroma.2017.04.014.

17. Wang W, Nema S, Teagarden D. Protein aggregation–pathways and influencing factors. Int J Pharm. 2010;390(2):89-99. https://doi.org/10.1016/j.ijpharm.2010.02.025.

18. Vázquez-Rey M, L DA. Aggregates in monoclonal antibody manufacturing processes. Biotechnol Bioeng. 2011;108(7):1494-508. https://doi.org/10.1002/bit.23155.

19. Liu HF, Ma J, Winter C, Bayer R. Recovery and purification process development for monoclonal antibody production. MAbs. 2010;2(5):480-99. https://doi.org/10.4161/mabs.2.5.12645.

20. Shukla AA, Hubbard B, Tressel T, Guhan S, Low D. Downstream processing of monoclonal antibodies–application of platform approaches. J Chromatogr B Analyt Technol Biomed Life Sci. 2007;848(1):28-39. https://doi.org/10.1016/j.jchromb.2006.09.026.

21. Toueille M, Uzel A, Depoisier J-F, Gantier R. Designing new monoclonal antibody purification processes using mixed-mode chromatography sorbents. J Chromatogr B Analyt Technol Biomed Life Sci. 2011;879(13-14):836-43. https://doi.org/10.1016/j.jchromb.2011.02.047.

22. Voitl A, Müller-Späth T, Morbidelli M. Application of mixed mode resins for the purification of antibodies. J Chromatogr A. 2010;1217(37):5753-60. https://doi.org/10.1016/j.chroma.2010.06.047.

23. Liu HF, McCooey B, Duarte T, Myers DE, Hudson T, Amanullah A, et al. Exploration of overloaded cation exchange chromatography for monoclonal antibody purification. J Chromatogr A. 2011;1218(39):6943-52. https://doi.org/10.1016/j.chroma.2011.08.008.

24. Stone MT, Cotoni KA, Stoner JL. Cation exchange frontal chromatography for the removal of monoclonal antibody aggregates. J Chromatogr A. 2019;1599:152-60. https://doi.org/10.1016/j.chroma.2019.04.020.

25. Dieter M, Rene Faber H-H Hörl WD, Stefan F-F, Miyako H. New HIC and AEX membrane adsorbers. https://bioprocessintl.com/downstream-processing/chromatography/hydrophobic-interaction-membrane-chromatography-for-large-scale-purification-of-biopharmaceuticals-184195/.

26. Kuczewski M, Fraud N, Faber R, Zarbis-Papastoitsis G. Development of a polishing step using a hydrophobic interaction membrane adsorber with a PER.C6-derived recombinant antibody. Biotechnol Bioeng. 2010;105(2):296-305. https://doi.org/10.1002/bit.22538.

27. Mehta KK, Vedantham G. Next-generation process design for monoclonal antibody purification. In: *Biopharmaceutical Processing*. 2018, 127. Elsevier; 793-811. https://doi.org/10.1016/B978-0-08-100623-8.00039-6.

28. Wang J, Zhou J, Gowtham YK, Harcum SW, Husson SM. Antibody purification from CHO cell supernatant using new multimodal membranes. Biotechnol Prog. 2017;33(3):658-65. https://doi.org/10.1002/btpr.2454.

29. Khanal O, Kumar V, Lenhoff AM. Displacement to separate host-cell proteins and aggregates in cation-exchange chromatography of monoclonal antibodies. Biotechnol Bioeng. 2021;118(1):164-74. https://doi.org/10.1002/bit.27559.

30. Khanal O, Kumar V, Westerberg K, Schlegel F, Lenhoff AM. Multi-column displacement chromatography for separation of charge variants of monoclonal antibodies. J Chromatogr A. 2019;1586:40-51. https://doi.org/10.1016/j.chroma.2018.11.074.

31. Brgles M, Clifton J, Walsh R, Huang F, Rucevic M, Cao L, et al. Selectivity of monolithic supports under overloading conditions and their use for separation of human plasma and isolation of low abundance proteins. J Chromatogr A. 2011;1218(17):2389-95. https://doi.org/10.1016/j.chroma.2010.11.059.

32. Chi EY, Krishnan S, Randolph TW, Carpenter JF. Physical stability of proteins in aqueous solution: mechanism and driving forces in nonnative protein aggregation. Pharm Res. 2003;20(9):1325-36. https://doi.org/10.1023/A:1025771421906.

33. Cromwell MEM, Hilario E, Jacobson F. Protein aggregation and bioprocessing. AAPS J. 2006;8(3):9. https://doi.org/10.1208/aapsj080366.

34. Gerstner JA, Cramer SM. Cation-exchange displacement chromatography of proteins with protamine displacers: effect of induced salt gradients. Biotechnol Prog. 1992;8(6):540-5. https://doi.org/10.1021/bp00018a011.

35. Natarajan V, Cramer SM. Optimization of ion-exchange displacement separations. J Chromatogr A. 2000;876(1-2):63-73. https://doi.org/10.1016/S0021-9673(00)00139-4.

36. Brooks CA, Cramer SM. Solute affinity in ion-exchange displacement chromatography. Chem Eng Sci. 1996;51(15):3847-60. https://doi.org/10.1016/0009-2509(95)00287-1.

37. Guiochon G. *Fundamentals of preparative and nonlinear chromatography*. 2. ed. Amsterdam: Elsevier Acad. Press; 2006.

38. Katti AM, Dose EV, Guiochon G. Comparison of the performances of overloaded elution and displacement chromatography for a given column. J Chromatogr A. 1991;540:1-20. https://doi.org/10.1016/S0021-9673(01)88795-1.

39. Felinger A, Guiochon G. Optimization of the experimental conditions and the column design parameters in overloaded elution chromatography. J Chromatogr A. 1992;591(1-2):31-45. https://doi.org/10.1016/0021-9673(92)80220-O.

40. Morbidelli M, Servida A, Storti G, Carra S. Simulation of multicomponent adsorption beds. Model analysis and numerical solution. Ind Eng Chem Fund. 1982;21(2):123-31. https://doi.org/10.1021/i100006a005.

41. Kaczmarski K, Mazzotti M, Storti G, Morbidelli M. Modeling fixed-bed adsorption columns through orthogonal collocations on moving finite elements. Comput Chem Eng. 1997;21(6):641-60. https://doi.org/10.1016/S0098-1354(96)00300-6.

Repository KITopen

Dies ist ein Postprint/begutachtetes Manuskript.